Morphometrics

Morphometrics is the branch of mathematics studying the metrical and statistical properties of shapes and shape changes of geometric objects like molecules, fossils, brains, bird wings, ancient handcraft, modern cars, etc.

Morphology includes the sub-disciplines of functional morphology, biomechanics, ecomorpholog~ and evolutionary morphology, and provides data for developmental biology, neurobiology, physiology, genetics, paleontology, behavior and systematics.

Does morphology "lead" or "follow" in the development of evolutionary theory?

On Growth and Form Sir D'Arcy W. Thompson, 1917 - The mathematization of natural history. Thompson comes out punching with an array of arguments and stresses the importance of understanding the natural world quantitatively, but is limited philosophically to descriptive and classificatory methods (although embryology had already embarked on experimental manipulation).

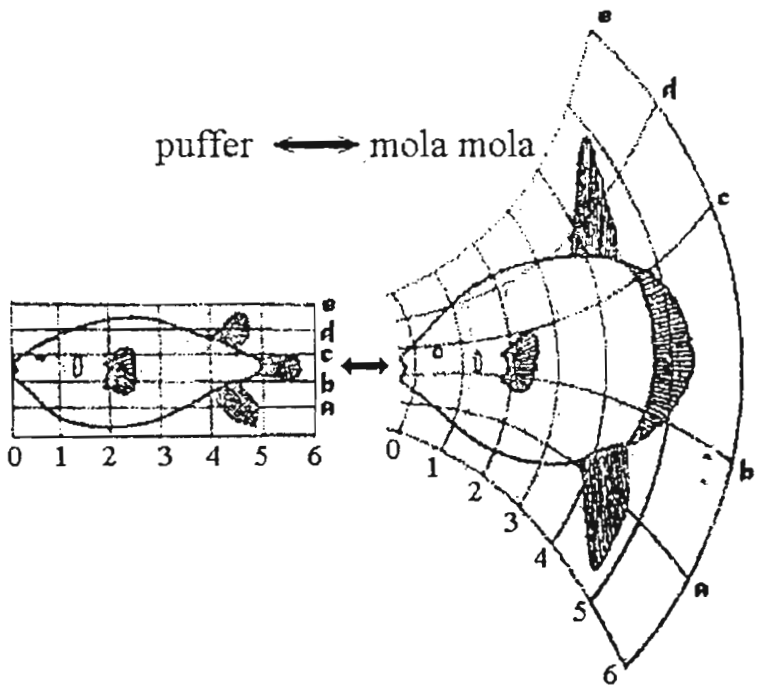

Univariant data plots (X) -- The distribution of the variance in character measurements should always be normally distributed, Data transformations -- why alter your data?

What to do? It may be that B is heterogenous, and if broken up into two OTU's might resolve the situation. This is not valid if the overlapping variation occurs within individual organisms or interbreeding populations. In the latter case, the situation must represent one of the five resolutions shown below, and the apparent statistical overlap is an artifact of inadequate sampling.

$\overline{A\ B\ C}$ $\quad \overline{A}\ \overline{B}\ \overline{C}$ $\quad \overline{A\ B}\ \overline{C}$ $\quad \overline{A}\ \overline{B\ C}$ $\quad \overline{A\ C}\ \overline{B}$

Bivariant data plots (X,Y) -- Correlations between morphological characters. Data exploration -- should I plot everything? Two morphological values can be combined into a single variable or ratio, Ratios are excellent for removing size, weight, etc. from a term, but what happens to the variance? Is it still normally distributed in the new term?

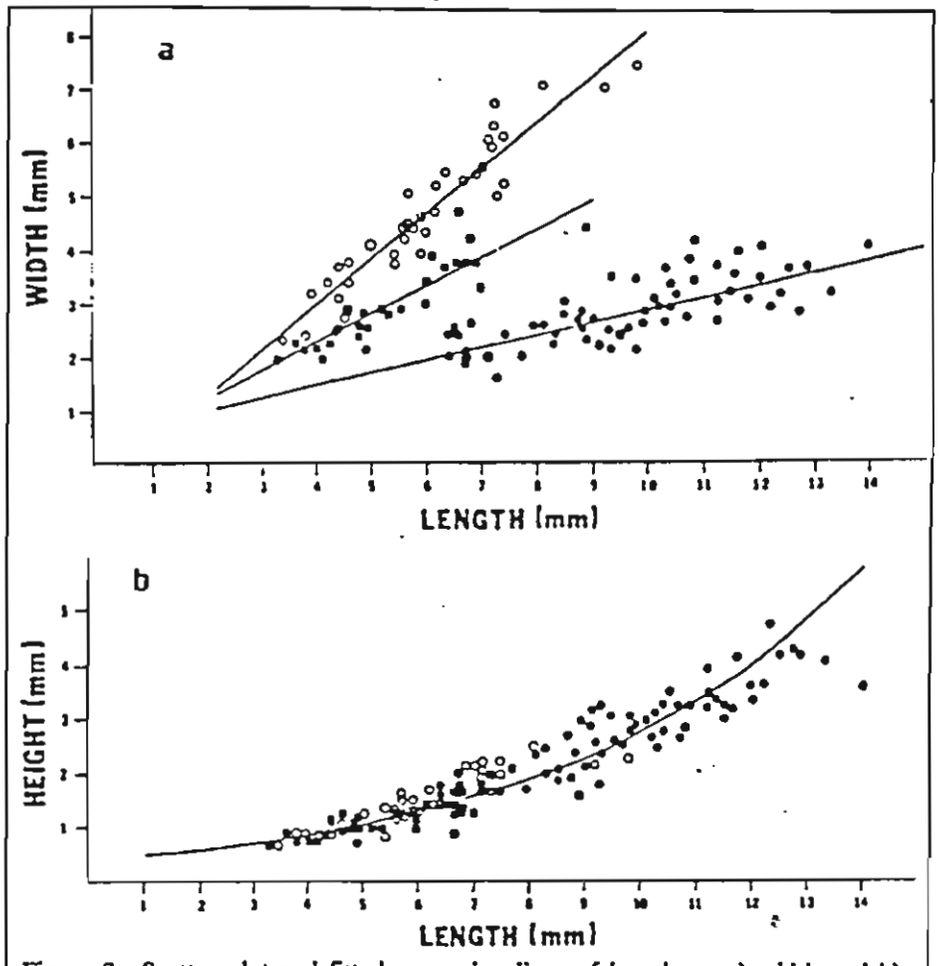

Figure 2. Scatter plot and fitted regression lines of length on a) width and b) height for three ecophenotypes ofthe marine plant limpet *Tectura depicta*. R^2 values: a) o = .5955, ■ = .8113, • = .8586; b) = .8662. Reprinted with permission from Bull. So. Calif. Acad. Sci., 81(2), 1982.

Procrustes analysis -- The shape of an object can be described by the coordinates of a set of well defined points or landmarks. Coordinate data from similar points across a group of individuals can be used to compare and contrast their shapes provided they have been superimposed (i.e., translated, rotated and scaled) in a common coordinate system In this coordinate system differences in the relative positions of the corresponding points on different configurations are directly reflected by the differences In their coordinates.

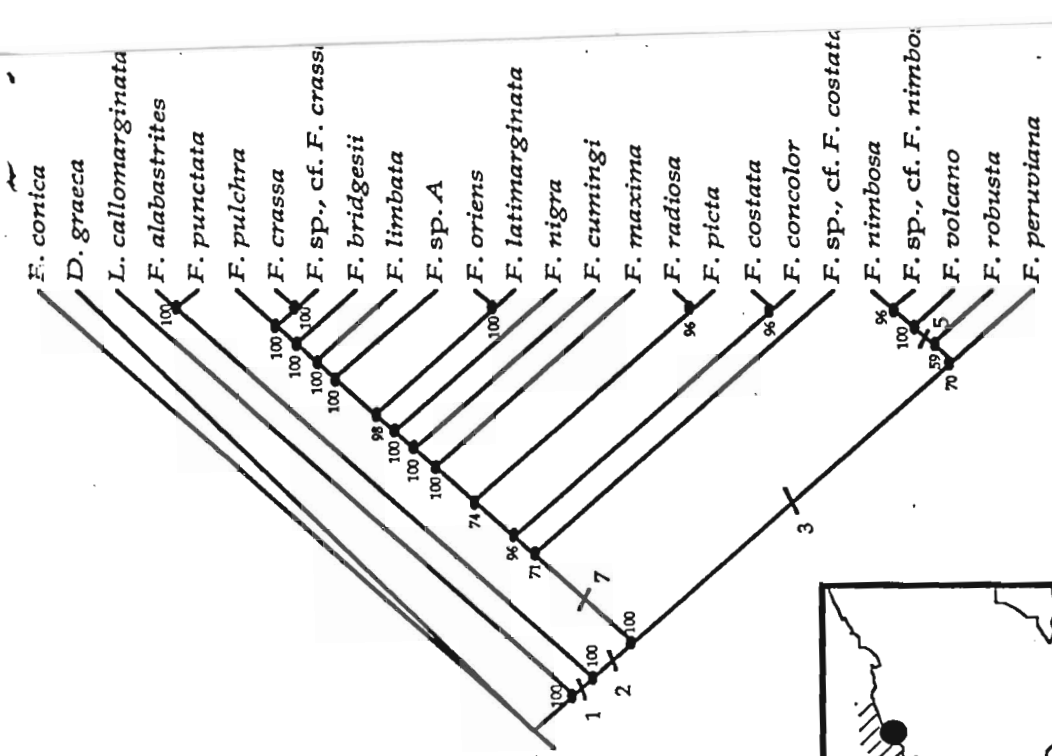

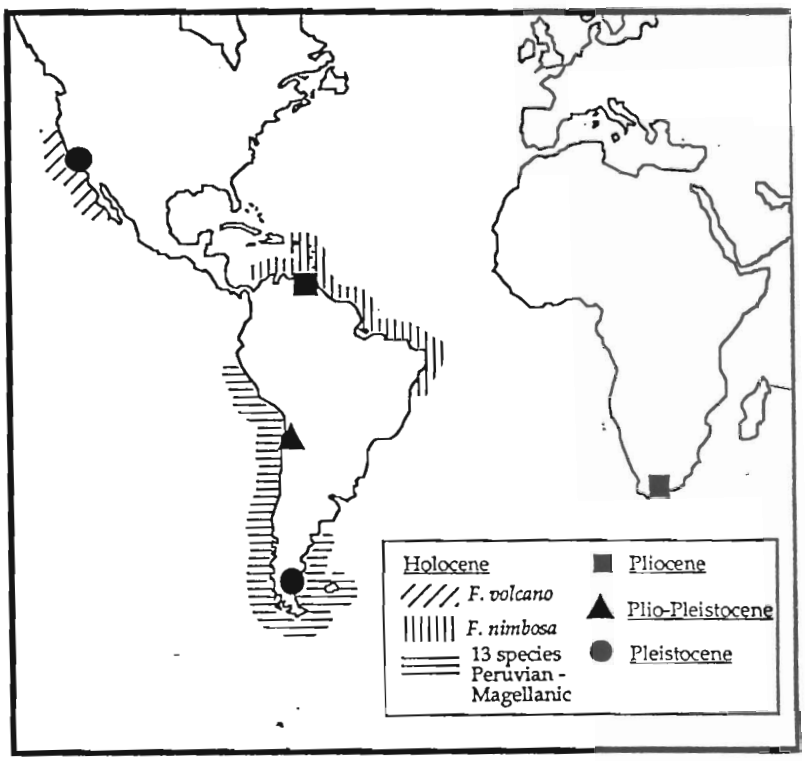

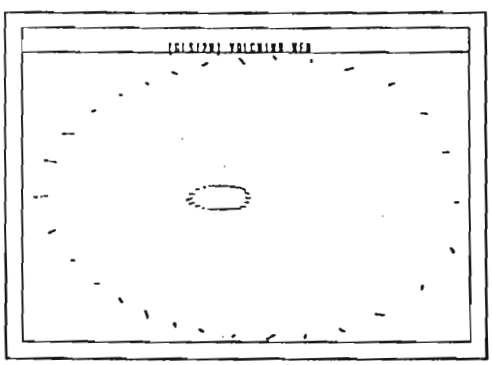

Figure 1 F. volcano and F. nimbosa

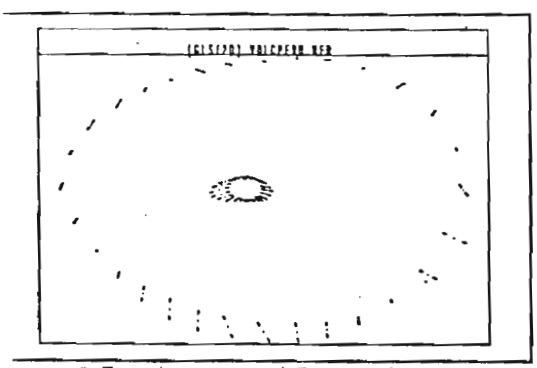

Figure 2 F. volcano and F. peruvianus

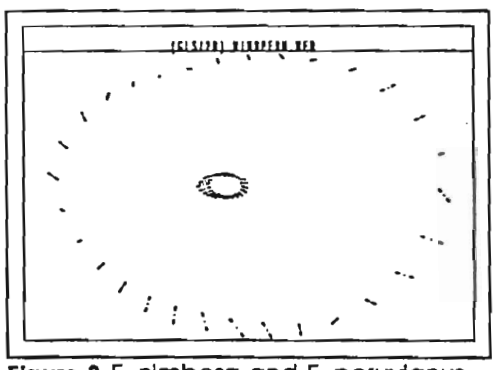

Figure 3 F. nimbosa and F. peruvianus

Multi-variant data plots (X,Y....n,n) -- Assumptions of multivariate normality required, but seldom demonstrated. Simple sums or means and sums of squares and cross-products (correlations or covariances) of raw or logged data over samples; or distances computed between individuals or centroids are the basic summary statistics of multivariate analyses. The vectors of these variables are easily represented In 2 and 3 dimensions and are extend to n dimensions, Principal components are variables whose values or scores represent linear or weighted combinations of the original variables, The weights or coefficients represent the cosines of the angles by which the axes are rotated.

Principal component analysis (PCA) has been a commonly used mathematical procedure that transforms a number of (possibly) correlated variables into a (smaller) number of uncorrelated variables called *principal components*. The first principal component accounts for as much of the variability in the data as possible (typically sized in our applications), and each succeeding component accounts for as much of the remaining variability as possible.

Principal component analysis is performed on Covariance (scaled sums of squares and cross products), or, Correlation (sums of squares and cross products from standardized data) matrices. A Correlation matrix is used when the variances of individual variates substantially differ or the units of measurement of the individual variates differ.

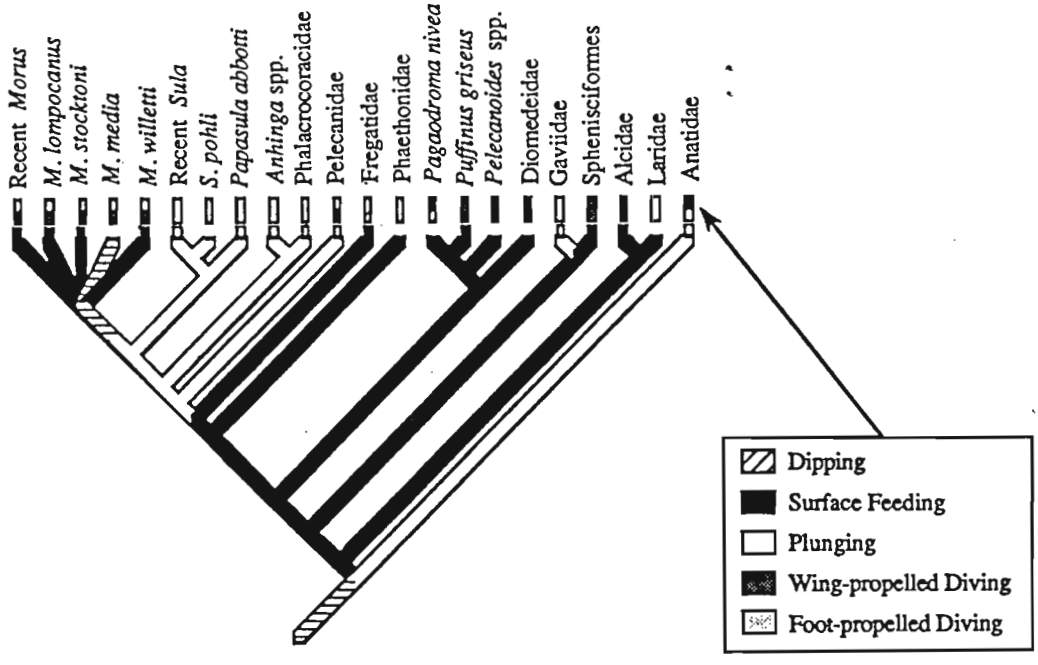

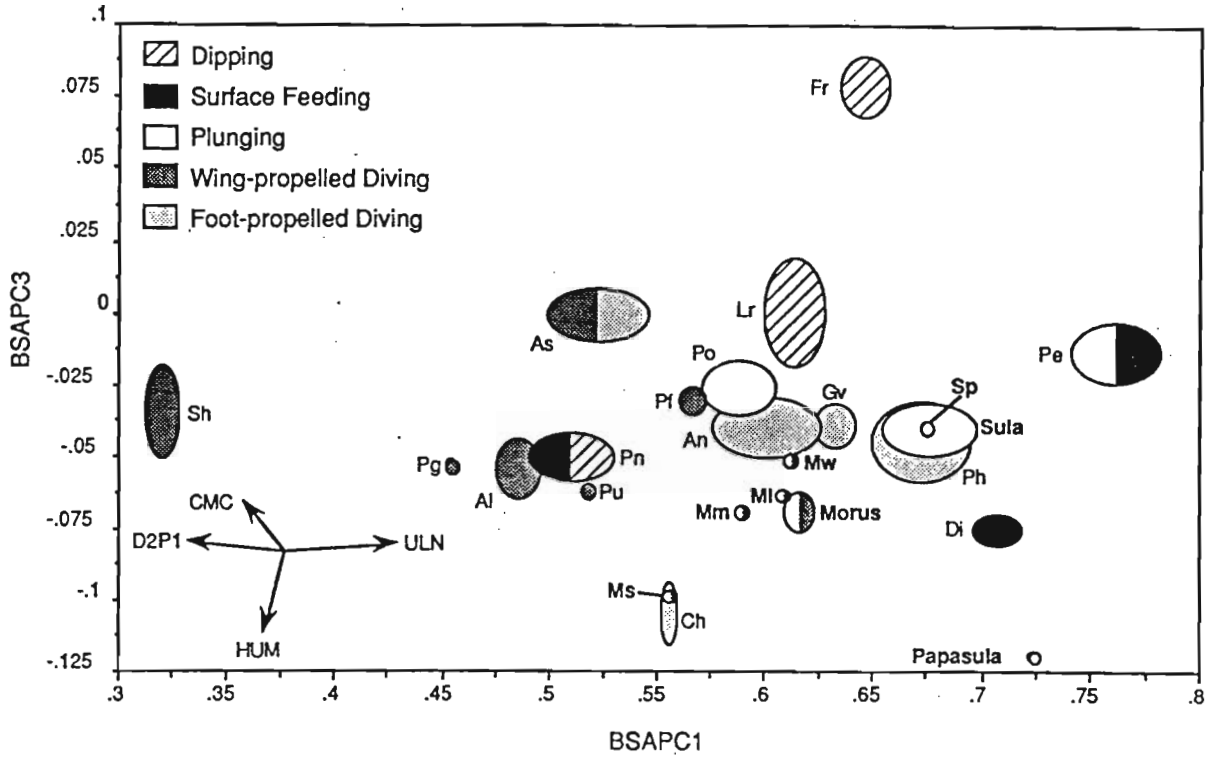

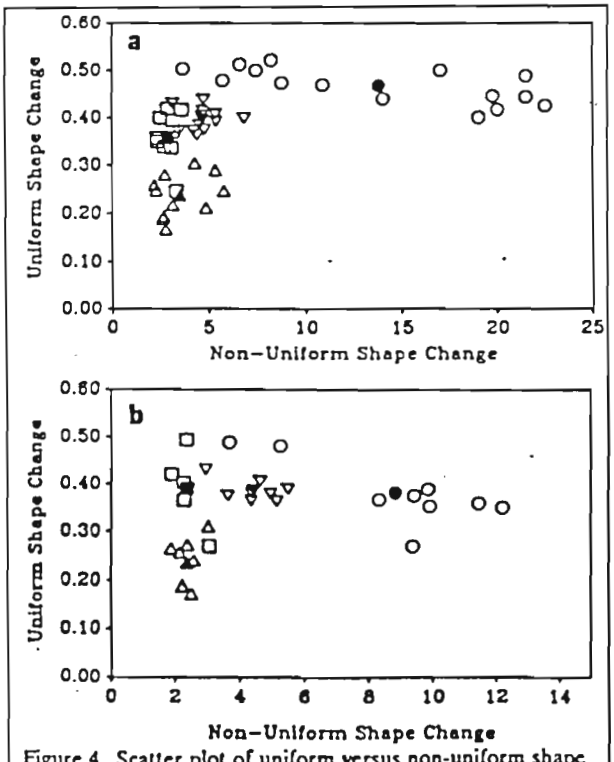

Figure 4. Scatter plot of uniform versus non-uniform shape change values for four nominal species of marine plant limpets from the Eocene of the Paris Basin. a) Data gathered with vernier calipers to the nearest 0.01 mm. b) Data gathered with the MorphoSys video imaging system. Open symbols: □ = *Patelloida arenarius*, o = *P.concavus*, ∇ = *P. elongata*, Δ = *P. pyramidale*. Solid symbols = means.

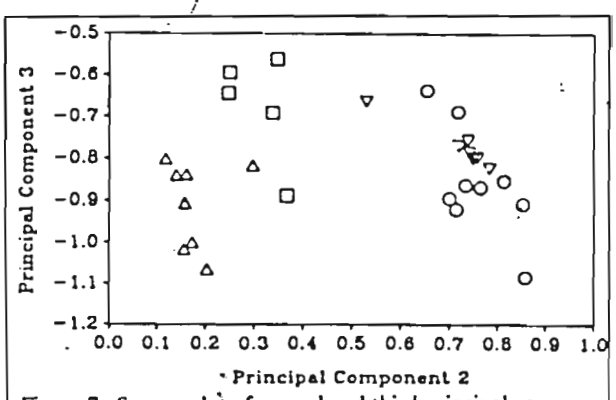

Figure 7. Scatter plot of second and third principal components scores from analysis of four nominal species of marine plant limpet from the Eocene of the Paris Basin. See Figure 4 for legend to symbols.

Table 3. Paris Basin Marine Plant Limpets: Eigenvalues of total log-transformed covariance matrix.

	Eigenvalues		% Total Variance		Cumulative % Total Variance	
Eigen-vectors	PCA	Burnaby	PCA	Burnaby	PCA	Burnaby
1	0.372	0.143	80.308	90.209	80.308	90.209
2	0.073	0.012	15.735	7.322	96.043	97.531
3	0.017	0.003	3.611	1.695	99.654	99.226
4	0.001	0.001	.263	.596	99.917	99.822
5	0.000	0.000	.062	.134	99.979	99.955
6	0.000	0.000	.017	.036	99.996	99.991
7	0.000	0.000	.004	.009	100.000	100.000
8	0.000	0.000	.000	.000	100.000	100.000
9	0.000	0.000	.000	.000	100.000	100.000

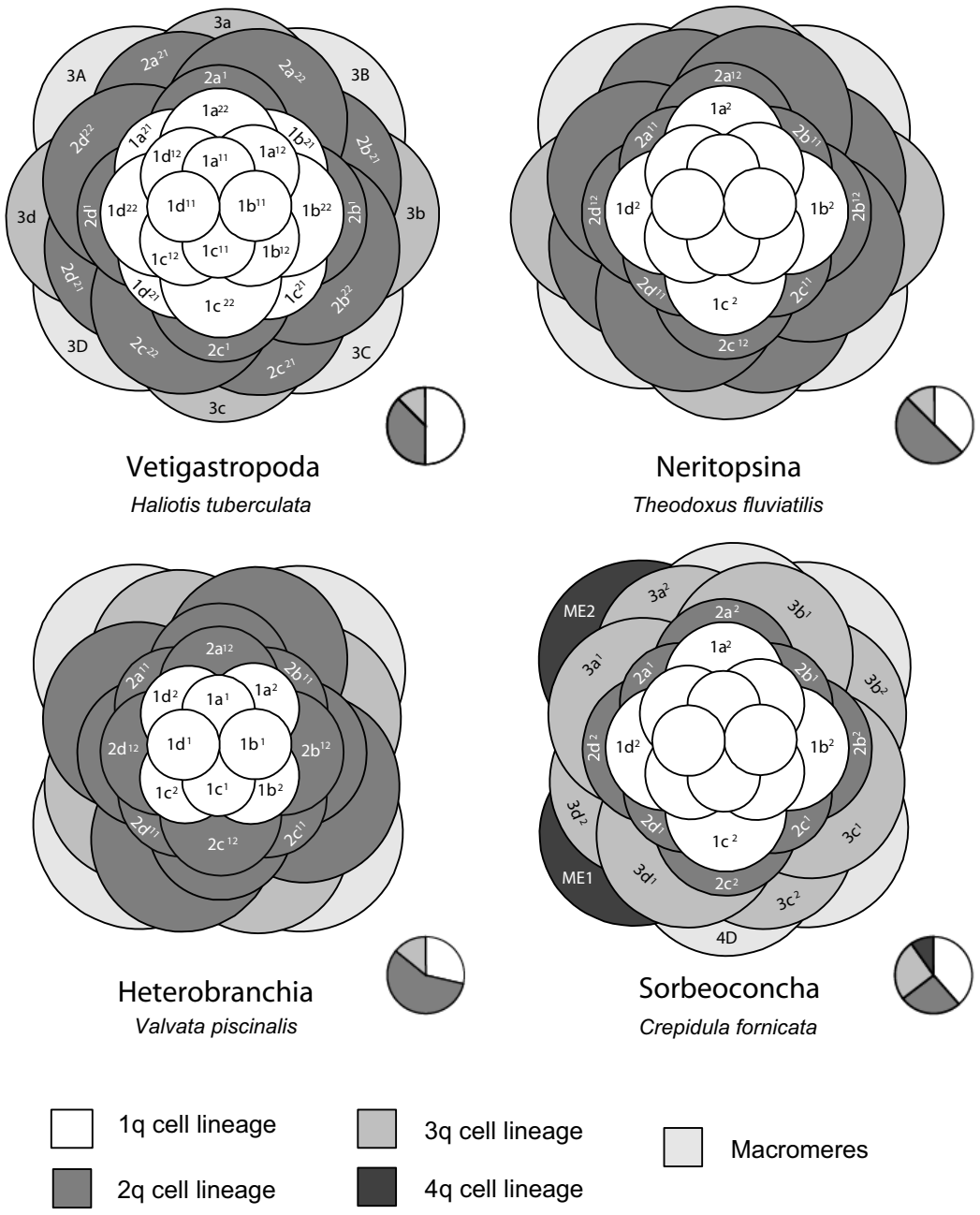

FIGURE 8. Stylized embryo composition at the 32-36 cell stage in four gastropod subclades – Vetigastropoda (36 cells), Neritospina (36 cells), Heterobranchia (32 cells), and the Sorbeoconcha (34 cells). All cells are labeled in the Vetigastropoda; in subsequent diagrams only cells whose identity has changed relative to the vetigastropod condition are labeled. Cells are shaded to show affinities as cell lineage descendents, and pie charts summarize overall embryo composition for each taxon. Cell lineage data from van den Biggelaar and Haszprunar (1996).

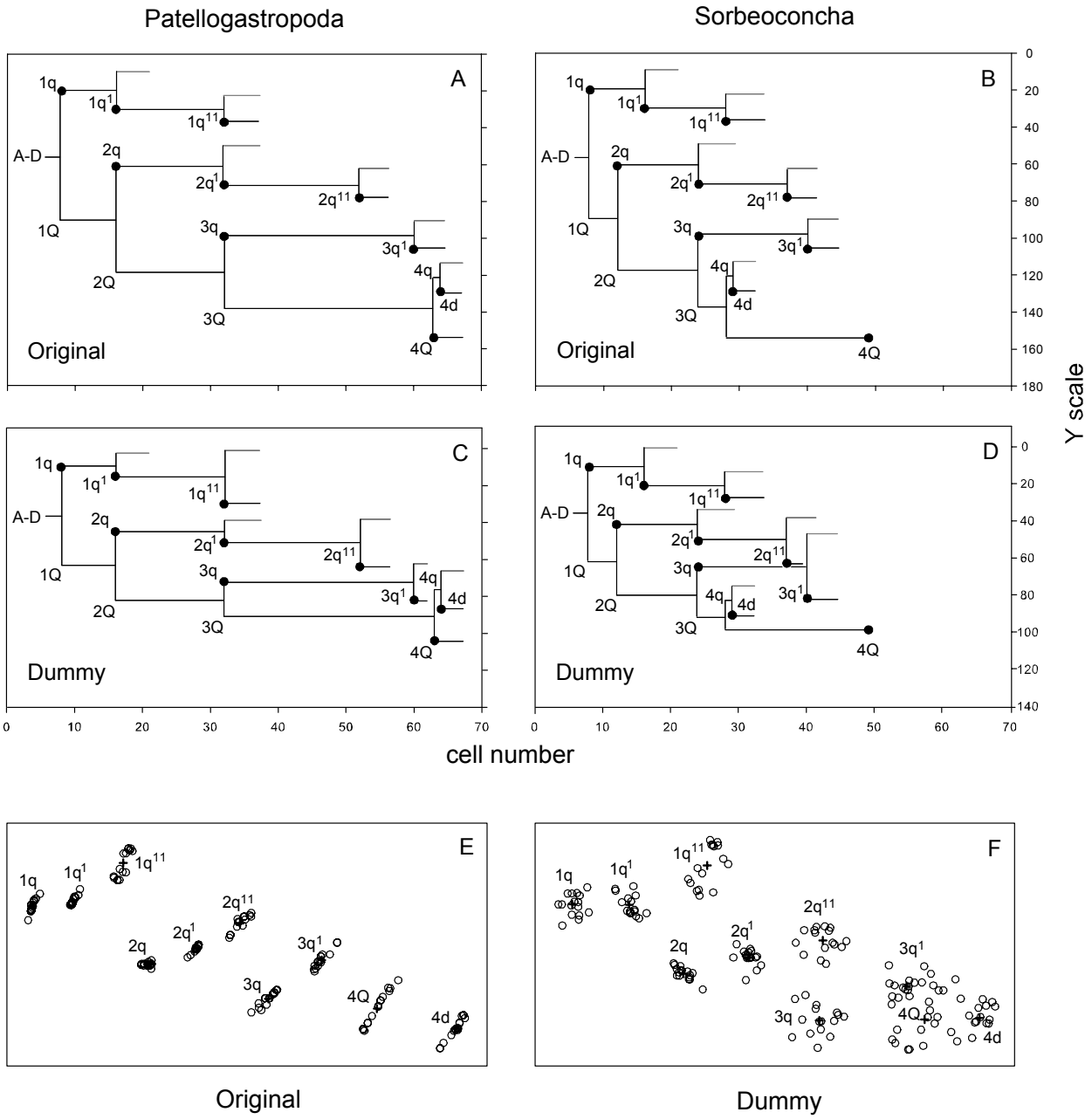

FIGURE 1. A-D. Cell lineage trees. Coding of cell lineage trees follows Conklin's (1897) notation for the designation of cell lineages. Here q represents the micromeres a, b, c, and d, whereas Q = macromeres A, B, C, and D (see Lindberg and Guralnick [2003]). Landmarks used in this study are marked by •. A. Original coding of the cell lineage tree for the Patellogastropoda. B. Original coding of the cell lineage tree for the Sorbeoconcha. Note that in the original coding the y values for each cell lineage are constant. C. Randomized (dummy) coding of the y coordinates for the Patellogastropoda cell lineage tree. D. Randomized (dummy) coding of the y coordinates for the Sorbeoconcha cell lineage tree. Note that in the dummy coding both x and y coordinates vary. E-F. Procrustes superposition plots. E. Original data with linear variation around means. F. Dummy data with circular variation around means.

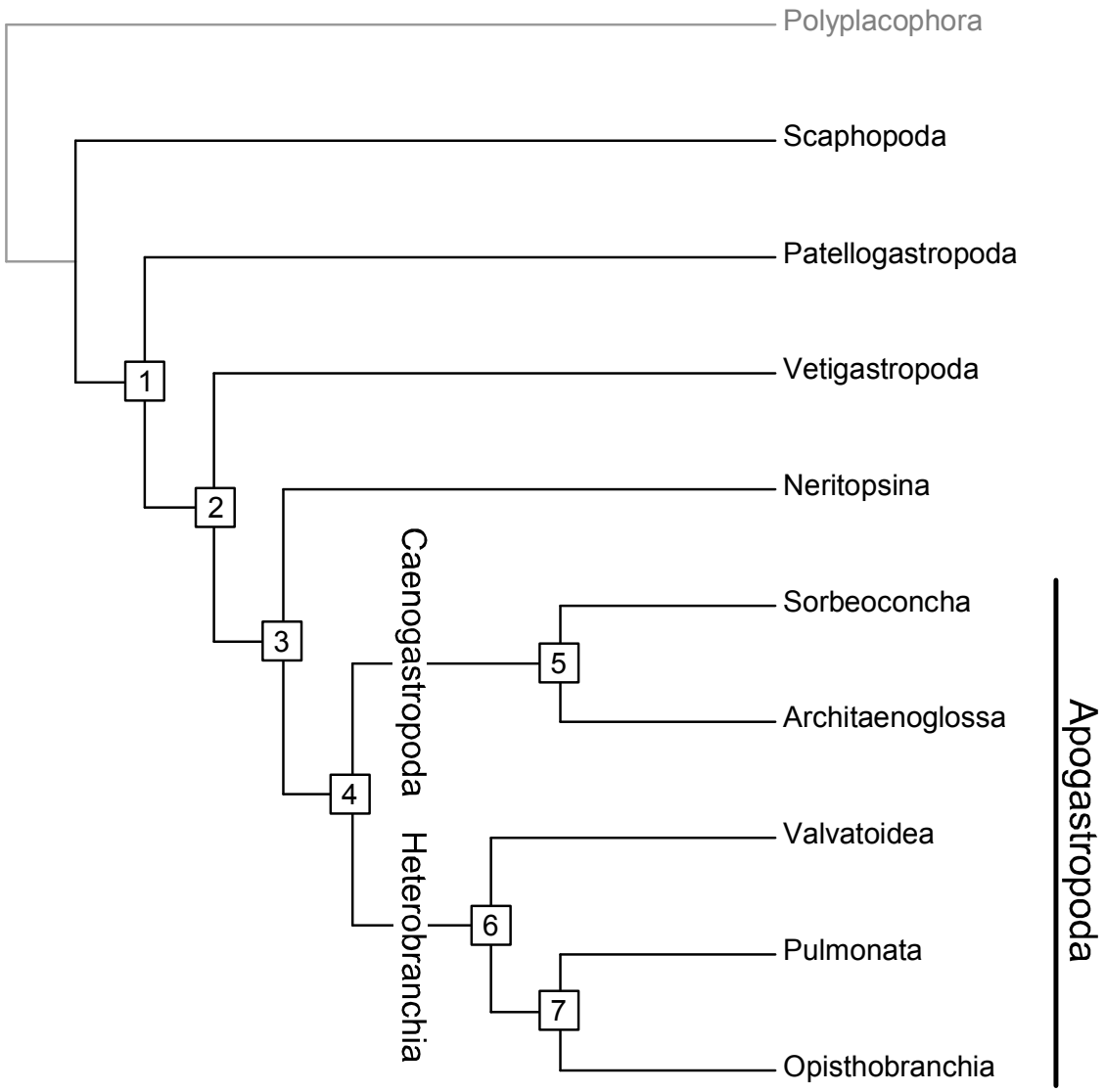

FIGURE 2. Hypothesized gastropod relationships and nomenclature used for tpsTree analysis, and character and Procrustes distance mapping. Tree is based on a strict consensus tree of three maximum parsimony trees. For details and statistics see Ponder and Lindberg 1997: Table 2; fig. 3b. Consecutive numbers refer to hypothetical taxon units (or HTUs).

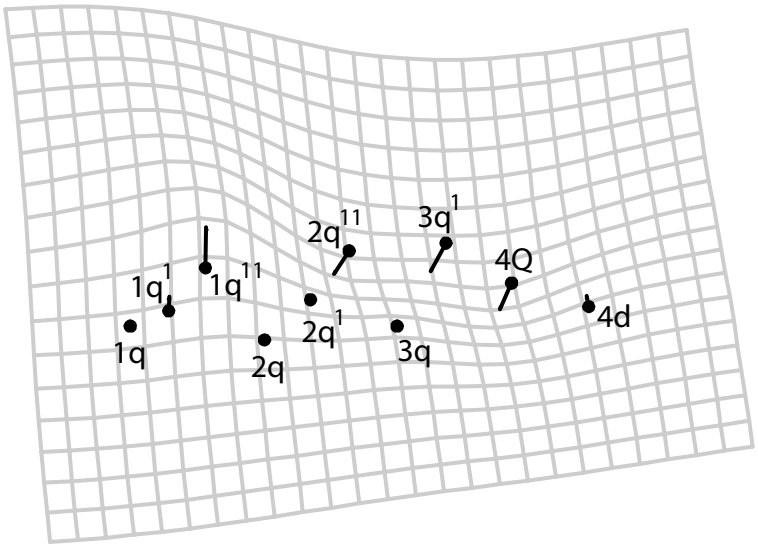

FIGURE 3. Deformation grid showing transformation of cell lineage tree from one configuration to another as calculated by a generalized Procrustes analysis. In the above example the starting coordinates of each of the ten cell lineages are represented by the solid circles and the alteration to their relative positions in the next configuration is represented by the vector. Trends present in the original data were used to verify the direction of timing change (acceleration or retardation) relative to the compression and expansion patterns of each grid. Cell lineage originations that are accelerating between OTUs or HTUs produce compressions in the grid ($2q^{11}$, $3q^{1}$, 4Q), while cell lineages that are decelerating between configurations cause expansion of the grid ($1q^{1}$ and $1q^{11}$).

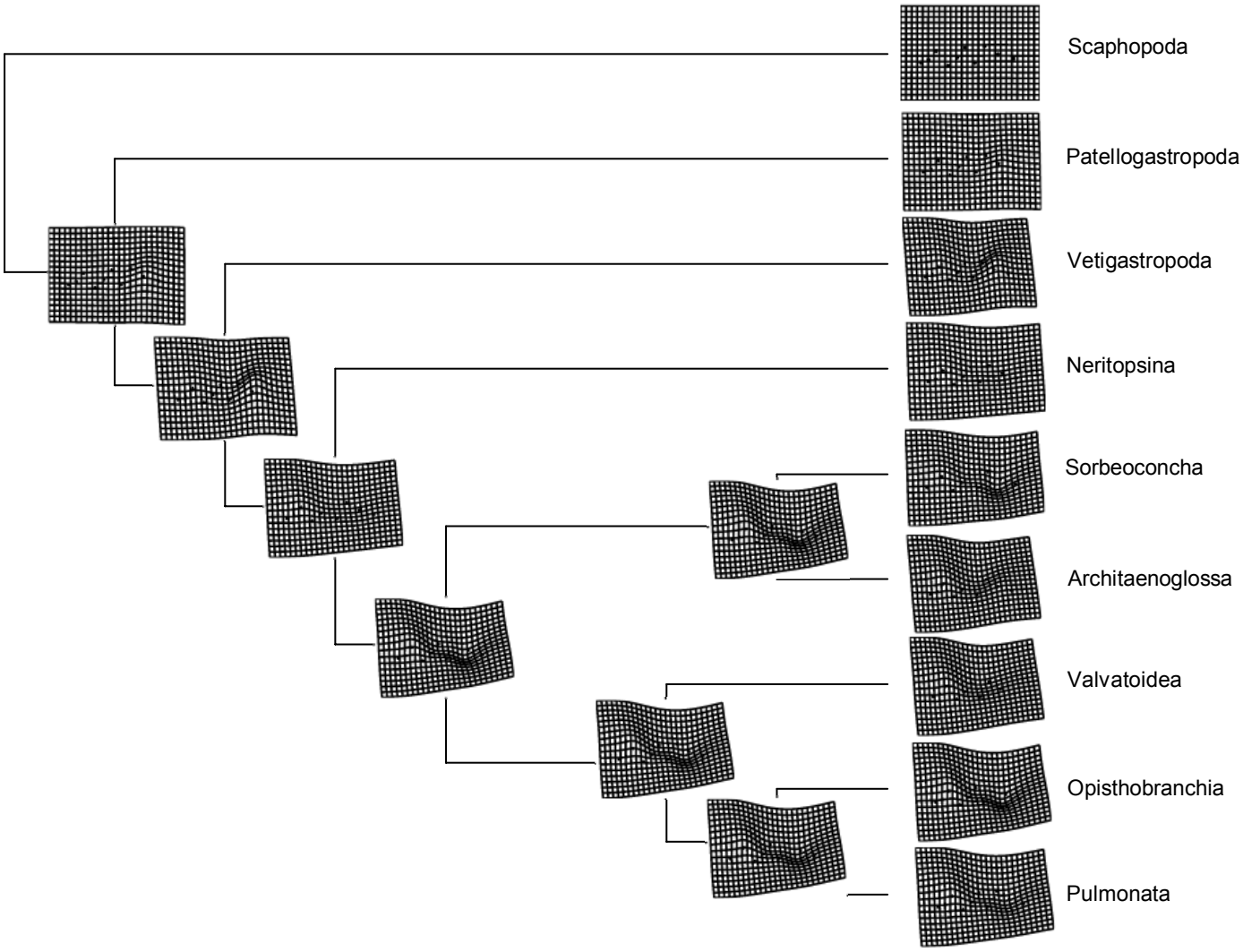

FIGURE 5. Deformation grids for eight major gastropod subclades, the outgroup Scaphopoda, and internal nodes plotted on the Ponder and Lindberg (1997) hypothesis of gastropod phylogeny. Reconstruct character states at HTUs calculated under maximum parsimony, accelerated transformation, and Dollo character ordering assumptions (see Table 1 for values).

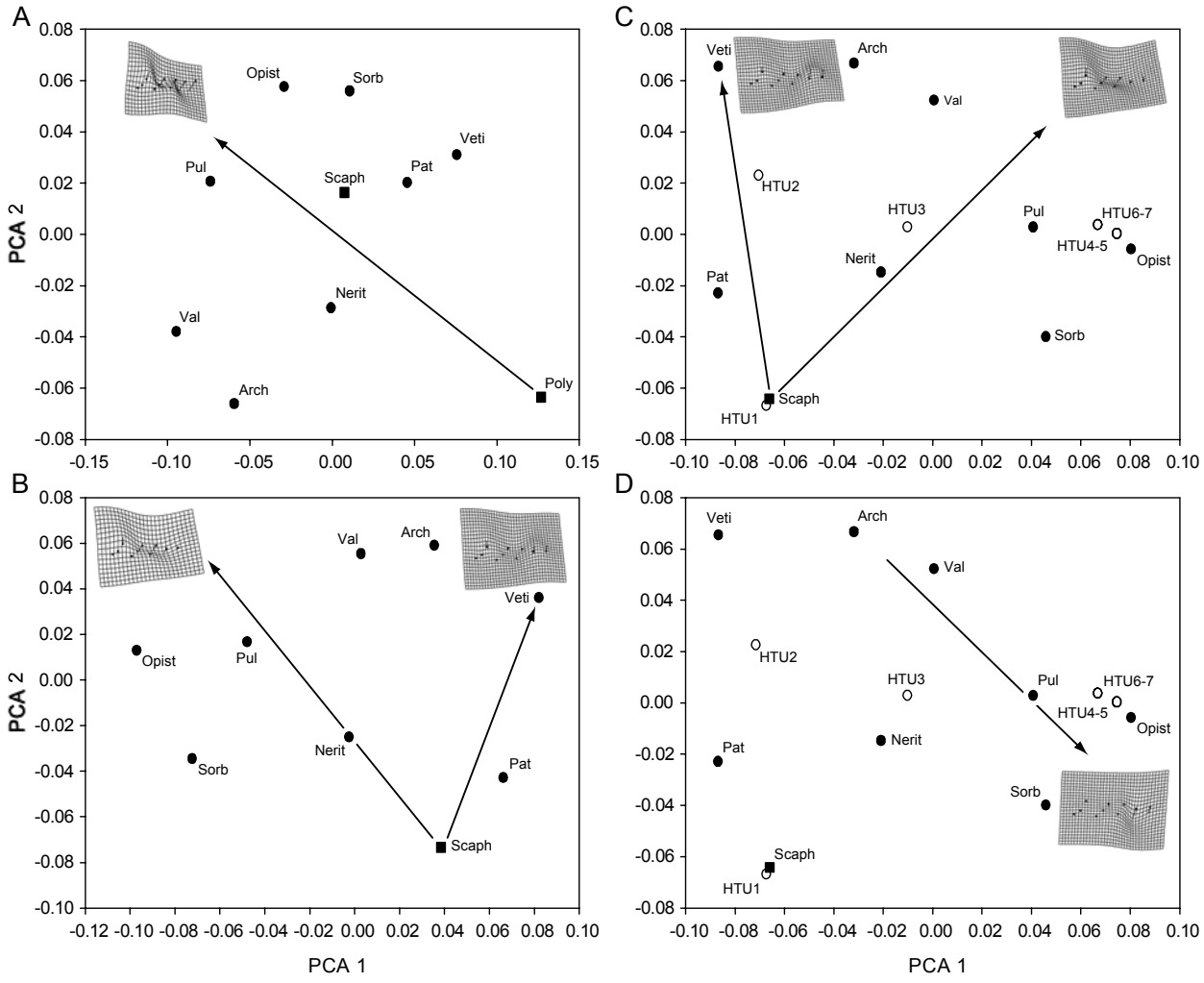

FIGURE 6. Principal component (PC) analysis of partial warp scores based on a generalized least squares Procrustes analysis of cell lineage data. A. Polyplacophora representing outgroup with implied change in PC space between Polyplacophora and Heterobranchia taxa. B. Scaphopoda as sole outgroup with deformation grids representing implied change in PC space between Scaphopoda and Vetigastropoda (right) and Scaphopoda and Heterobranchia taxa (left). C. Scaphopoda as outgroup with deformation grids representing implied change in PC space between Scaphopoda and Vetigastropoda (left) and Scaphopoda and Heterobranchia taxa (right). D. Same as C, but with deformation grid representing implied change in PC space between Valvatoidea and Architaenoglossa taxa and their sister taxa Sorbeoconcha and Opisthobranchia+Pulmonata respectively. Outgroups = ■, Ingroups = ●, and HTUs = ○.

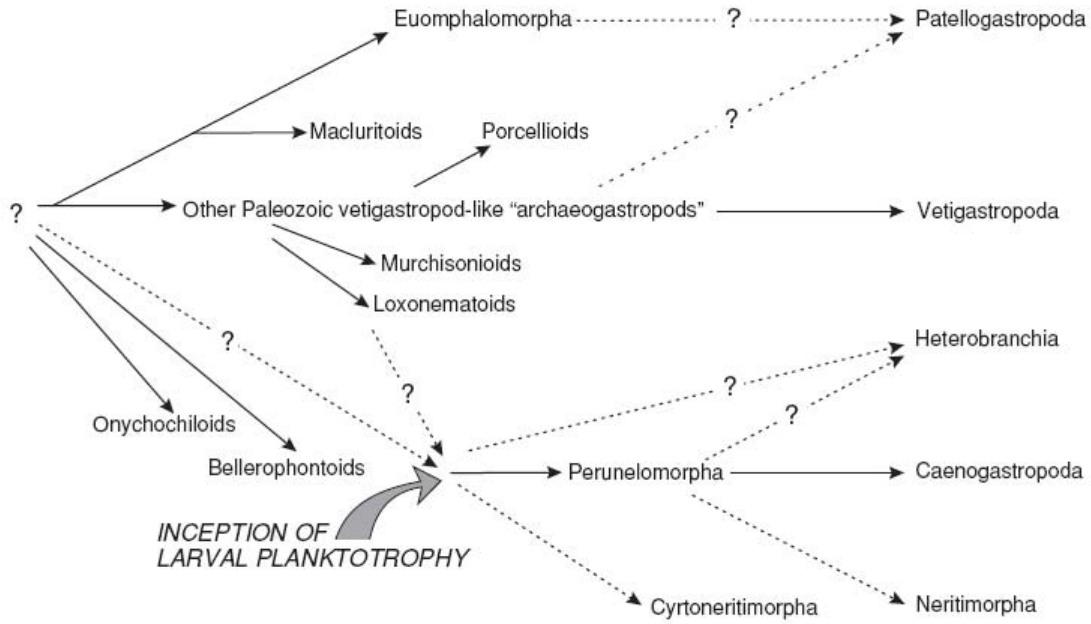

FIGURE 10.3. Phylogenetic hypothesis on phylogeny of the Paleozoic gastropods inferred from protoconch morphology based mainly on Frýda and Manda (1997), Frýda and Bandel (1997), Bandel and Frýda (1998, 1999), Bandel (1997, 2002a, b), Frýda and Blodgett (1998, 2001, 2004), Frýda (1999a, d, 2001), Nützel *et al.* (2002), Nützel (2002), and Frýda and Rohr (2004, 2006) (see text for discussion).